

Article

Archaeological and Archaeometric Insights into a Roman Wall Painting Assemblage from the Blanes Dump (Mérida)

Gonzalo Castillo Alcántara ¹, Daniel Cosano Hidalgo ^{2,*}, Alicia Fernández Díaz ³
and José Rafael Ruiz Arrebola ^{2,*}

¹ Department of Art History, Archaeology and Music, University of Córdoba, 14071 Cordoba, Spain; aa2caalg@uco.es

² Department of Organic Chemistry, Institute of Chemistry for Energy and the Environment Instituto (IQUEMA), Faculty of Science, Patricia Unit for R&D in Cultural Heritage, University of Cordoba, 14071 Cordoba, Spain

³ Department of Prehistory, Archaeology, Ancient History, Medieval History and Historiographic Sciences and Techniques, University of Murcia, 30003 Murcia, Spain; aliciafd@um.es

* Correspondence: q92cohid@uco.es (D.C.H.); qo1ruarj@uco.es (J.R.R.A.)

Abstract: In this paper we describe the archaeological and archaeometric analysis of a Third Pompeian Style assemblage from the Blanes dump in Mérida (Spain). Based on the pottery context, the material would have been part of the decoration of a public or private space remodelled towards the end of the 1st century AD. Several samples from the middle area of the assemblage, including panels, inter-panels and a frieze, were selected and studied using X-ray diffraction (XRD), X-ray fluorescence (XRF), Raman, gas chromatography and petrographic analysis. The results revealed the use of hematite, cinnabar, minium and goethite in different panels, as well as goethite, Egyptian blue, calcite, glauconite and carbon for the decorative motifs. They allowed us to define the painting techniques used and how they have affected the degradation of the pigments.

Keywords: Augusta Emerita; Roman wall painting; third Pompeian style; mortar; pigment; Raman; cinnabar; minimum; thin section



Citation: Castillo Alcántara, G.; Cosano Hidalgo, D.; Fernández Díaz, A.; Ruiz Arrebola, J.R. Archaeological and Archaeometric Insights into a Roman Wall Painting Assemblage from the Blanes Dump (Mérida). *Heritage* **2024**, *7*, 2709–2729. <https://doi.org/10.3390/heritage7060129>

Academic Editors: Georgios P. Mastrotheodoros, Anastasia Rousaki and Eleni Kouloumpi

Received: 6 May 2024
Revised: 20 May 2024
Accepted: 22 May 2024
Published: 27 May 2024



Copyright: © 2024 by the authors. Licensee MDPI, Basel, Switzerland. This article is an open access article distributed under the terms and conditions of the Creative Commons Attribution (CC BY) license (<https://creativecommons.org/licenses/by/4.0/>).

1. Introduction

Augusta Emerita (present-day Mérida) was one of the most prominent enclaves of Roman Hispania due to its importance from the early Empire as the capital of Lusitania province. Proof of this can be seen in the extensive archaeological heritage recovered since the last century that has allowed the town's history to be revealed from its foundation to late antiquity [1] (Figure 1). Roman mural painting is no exception, and the studies undertaken in recent decades have allowed us to improve our knowledge of the insertion and development dynamics of decorative fashions and the craftsmanship of Italian and local workshops. The contribution of finds from waste dumps and fill levels has been of particular importance to our knowledge of urban remodelling processes and pictorial productions [2–4].

Historical-archaeological studies have been complemented in recent years with physicochemical analyses of mortars and pigments, looking in-depth at issues related to craftsmanship, execution techniques, recipes and resource collection. This corresponds to an interest in undertaking comprehensive studies that are supported by the development of sampling criteria and the definition of archaeometric techniques useful for characterising Roman mural painting [5–9].

In this regard, the case under study is an example of particular relevance to painting from Augusta Emerita, in that various ways of applying pigments in the same assemblage have been attested, as well as their effect on its state of conservation. This analysis has allowed us to delve more deeply into both the craftsmanship and the socio-economic status

of the property owner as well as to compare the results with information from the sources, including Pliny (Natural History, XXXIII) and Vitruvius (De Architectura, VII).



Figure 1. Satellite map of Spain with location of Augusta Emerita and current area photo.

1.1. The Archaeological Context

The rubbish dump on Almendralejo Street, known as the Blanes dump, is the largest of its type documented in Mérida. It reflects the town's construction and social dynamics between the 1st and the 5th centuries AD. The site was studied between 2005 and 2007 as a result of earth movements carried out in the so-called Corralón de los Blanes, a plot of land of more than half a hectare at 41 Almendralejo Street destined for the construction of a housing block and car parking.

The plot is located between Almendralejo Street and Marquesa de Pinares Avenue. The archaeological site is in its northern part, which in Roman times would have been extramural but at the foot of the Roman wall. It was a suburban area, and, therefore, it is not unusual to find rubbish dumps that would have been easily accessed for the disposal of urban waste [10]. This aspect is corroborated by the possible presence of a gate in the town walls on Almendralejo Street connecting to the road leading to the town of Toletum [11].

The archaeological excavation revealed a superposition of dumping that filled part of the exterior elevation of the wall to a depth of 11 m at some points. This caused the alteration of the area in urban and defensive terms, documenting the covering of various

industrial buildings, road infrastructure and funerary towers of a similar typology to those preserved in the Columbarium area. All this is evidence of the complex urban transformation that took place [10] (Figure 2).

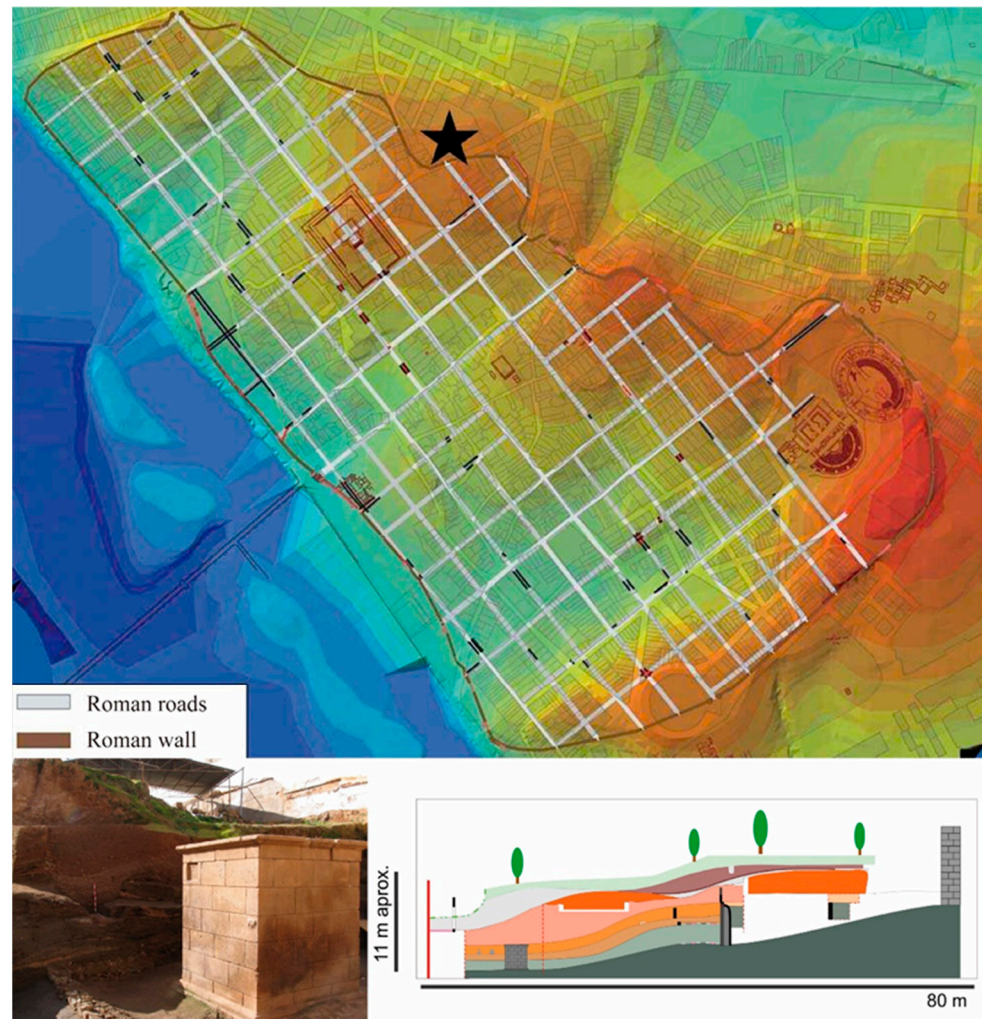


Figure 2. Above, planimetry of the Roman city and location of the Blanes dump. Below, section of the dump and photo of one of the funerary monuments (design based on Heras Mora, Olmedo Grajera and Pérez Maestro, 2017).

Prior to the site being used as a dump, the area was occupied by various routes. One can be distinguished leading to the Albarregas River. It is interpreted as a *via sepulchralis* with two monumental funerary structures on its sides, which sit on a possible levelling stratum dated to around the turn of era [12,13]. The finds identified in their interior date them to between the reigns of Tiberius and Claudius, a chronology similar to that established for the Columbarium mausoleums [14]. This is a clear indication that the subsequent dump began to develop in the middle of the 1st century AD.

At the beginning of the 60s of the 1st century AD, the enclosure and the mausoleums were filled to the top with solid waste that included building rubble and domestic rubbish. This created a regular surface on which the pre-existing paths were renewed, maintaining the funerary nature of the area and the morphology of the precinct [13]. At an undetermined time in the second half of the century, the area was once again occupied with cremation burials and monumental markings, although, in the 2nd century AD, the dumping of waste and building materials that maintain the landfill function are once again documented [13, 15]. Beginning in the 3rd century AD, the site saw continuous dumping of rubbish and rubble, leaving the original topography completely altered in the 4th century AD [13].

In contextual terms, the various units in which we were able to identify the fragments that make up the assemblage under analysis (UUEE 785, 985, 1437, 1470, 1471 and 1537) date to between 80 and 90 AD, based on the presence of water bottle sherds in Bracarense pottery, DR 4, 11, 17 and 18 lamps and the rim of a De Tommaso 42 unguentarium [2]. This date must be taken as a *terminus ante quem* for the execution of the assemblage, to which we must add the necessary existence of a time margin between its completion and its replacement.

1.2. Technical-Descriptive Analysis

Despite not knowing the original context to which the assemblage is associated, the fragments allow a clear reading of the compositional scheme of the middle zone from which to carry out the sampling of the various elements that make it up. They reveal a scheme of panels and inter-panels. In the former, a single fragment is found with remains of a motif that would have occupied the central part, although it is very worn and impossible to identify. Some fragments of the inter-panels define two different models. From the first we have part of the upper left corner of a panel and part of the inter-panel with a white scroll that could be part of some type of vegetal candelabra, as well as pairs of drops arranged on both sides of the fillet that separates the panel and inter-panel (Figure 3A). Beginning from the volute, which is usually represented in groups of two, the inter-panel would have been between 15 and 20 cm wide.

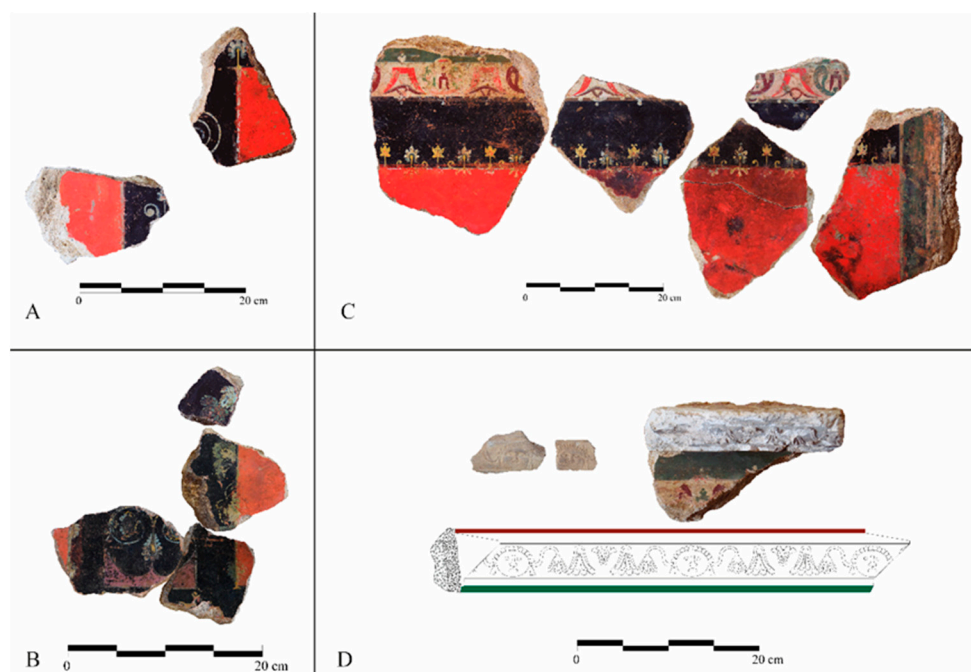


Figure 3. (A) Fragments of the first inter-panel with drop decoration and “V” elements. (B) Fragments of the second inter-panel with vine leaves, thyrsus and pine cones. (C) Fragments of the upper edge of the panels and Egyptian frieze. (D) Fragments of cornice and profile drawing.

The rest of the fragments belong to the lower closure of the second inter-panel, which is about 17 cm wide. The lower part shows a black field, probably from a predella at least 3.5 cm high; on it can be seen the remains of a yellow, white and red element on which a small yellow spiral rests. Above, the lower part of the inter-panel is preserved. It bears a motif composed of a violet band with a white border, rectangular on its lower side and with two concave semicircular spaces on the upper side. Above the vertex generated between the semicircles rises a palmette composed of a yellow stem surrounded by a blue line with blue drops. At the top of the stem, yellow spirals emerge that turn blue halfway through their development, ending in a flower with yellow and blue drops. On the edges of the two

panels arranged next to the inter-panel, pine cones and green vine leaves sprout on a fillet like a thyrsus, and, in the lower corner of one of the panels, a small horizontal yellow line like a metal foot can be seen. (Figure 3B).

The panels would have been delimited at their upper end and on one or two of their sides by a white fillet. On the upper side, these give way to a black field 10 cm high as a band that constitutes a continuation of the bottom of the inter-panels. In this, a decoration is developed that acts as the upper finish of the panels, composed of an alternation of two motifs (Figure 3C). The first is composed of a yellow stem with a blue drop and a white line with downward drops. Above it is topped by a small yellow leaf with five points in the shape of a star with a red line in the middle and two drops crowning the top. The second has a truncated conical base with a green line on the inside finished with spirals on the sides. From the central part emerges a yellow stem surrounded by small blue and white leaves.

The middle zone is completed with a frieze composed of a brownish fillet, a white band and a green band, which also extends along the sides of the wall, enclosing the whole at its ends. On the white band there is an alternation of two motifs. The first is composed of a red "M" motif with two reddish-brown and dark blue strokes, with another curved motif between them creating a schematic eye shape and finishing downwards with white drops. The upper part is finished with a small white cord-shaped motif and a drop. The second motif is composed of three quarters of a circle facing upwards whose ends retract vertically into the interior background. In the middle there is a green "M" motif with elongated arms with a small bifolium crowned by a drop and, below, a small cord-shaped motif. This alternates in its chromaticism with the first motif, so that in some cases the exterior is burgundy-red and the interior is green and in others it is the opposite. Finally, below, it is finished off by an oval drop with a burgundy-red core, another white drop below and, at the top, an oval drop with a bright red core and another above.

Fragments of the cornice that encloses the assemblage are preserved. It is composed of a small listel and a band with small female masks with headdresses and a triangular slope, from which two curved stems topped by a type of trefoil extend to the sides. Between each mask a motif develops composed of two multi-lobed buds facing downwards and a central, smaller one facing upwards. Above, a small listel gives way to an inclined section on which there are the remains of an upper area of which only a red trace is preserved (Figures 3D and 4).

It seems that all the backgrounds were painted using the fresco technique and the fillets, bands and motifs were executed subsequently when it was dry, as can be seen from the numerous losses we find in the upper part of the panel. Various fragments present differences in the pigments used for the panels, two types of red and yellow, a matter we will address below. On the cornice, there are no marks that indicate the separation between motifs due to the application of the mould, so it is possible that they were all made by chiselling. In the mortar, there is a finishing layer and three preparatory layers whose thickness ranges from between 0.4 and 1.7 cm, with a brownish tone and small and medium-sized aggregates, as well as a herringbone back. The cornice has a finishing layer and three preparatory layers with a more greyish tone, between 0.4 and 1.6 cm thick, with small and medium-sized aggregates, except for the first, which is highly refined.

1.3. Compositional and Ornamental Study

Although only one element of the predella ornamentation remains, making any type of analysis impossible, it constitutes a characteristic of the Third Style productions, being barely identified in the Fourth. We see this also in Vaison-La-Romaine; the room (u) in the Place Jules-Formigé *domus* in Fréjus; the room (S4) of the Maison de Nones de Mars in Limoges; Cave Pinel in Périgueux [16] in France; and Room (H. 27) of *Domus 3*, Insula 1 in Bilbilis [17] in Spain, among others.

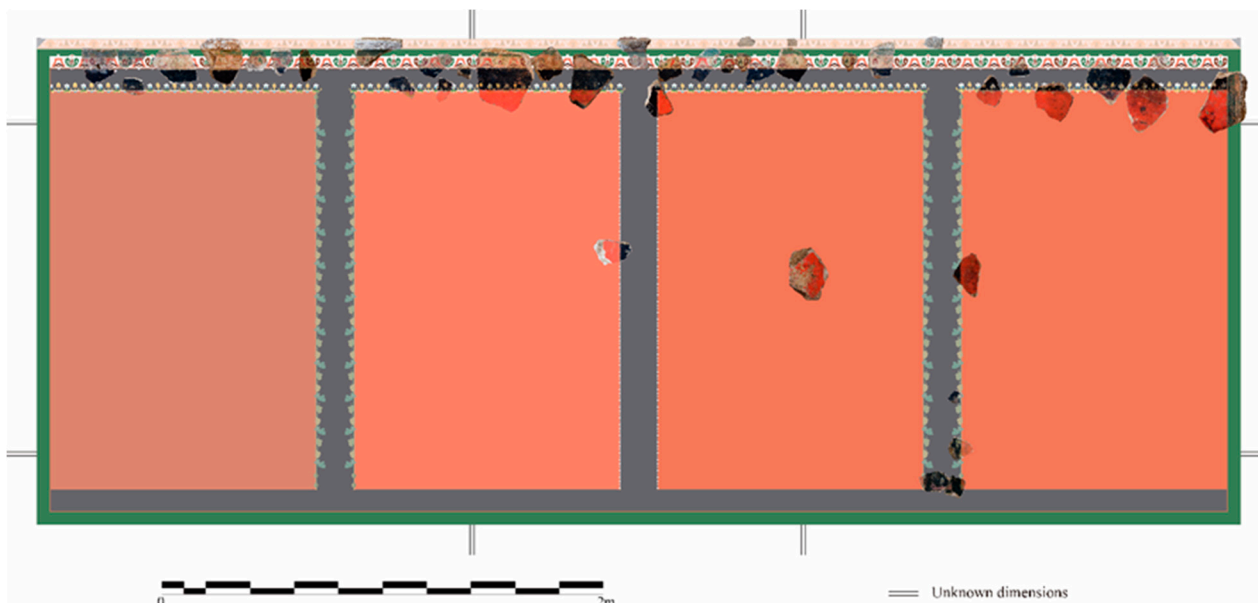


Figure 4. Hypothetical restitution of the assemblage.

Given that the panels do not present any interior element that can be analysed, we will first focus on the study of the inter-panel. In the first, the use of drops on both sides of the fillet that separates it from the panel is a characteristic motif of the Third Style that has lost the “V” elements, since the drops alone are not documented. We can refer to parallels such as the oecus (6) and tablinum (n) of the House of Trebius Valens (III 2, 1) [18], the cubiculum (f) in the House of Paquius Proculus (I 7, 1) [19] or a fragmentary group from the House of the Golden Bracelet (VI Ins. Occ., 42) [20] in Pompeii. In the provinces, it is documented at Cave Pinel in Périgueux [16], in the Vésone *domus* in the same town [21] and in the room (II) of the *domus* on Rue Paul-Deviolaine in Soissons [16]. In Hispania, we can include the cases of Can Terrés [22], the room (H. 27) of *Domus* 3, Insula 1 in Bilbilis [17], those of Celsa [23] or that of Del Ángel Street in Cartagena [24].

The data suggest the existence of a vegetal candelabra on the second inter-panel, although we cannot specify its shape. However, it is possible to point out some parallels, such as that of the atrium (b) of the House of Casca Longus (I 6, 11), where we see the same motif with a rectangular base, dated to the Third Style [25]. We find a similar form in the *domus* on Via Sigismondo in Rimini, also in the lower part of an inter-panel next to a predella [26]. The presence of the thyrsi with pine cones and vine leaves on the edges of the panel represents an element that was highly developed in the production of the Third Style, typical of the Bacchic repertoire. Although we do not observe a similar arrangement for the vine leaves in other examples, we do see it with the pine cones in the cubiculum (5) of the House of M. Lucretius Fronto (V 4, a) [27] and in the Vésone *domus* in Périgueux [21].

On the upper sides of the panels, the chromatic and figurative opulence are in keeping with the Phase IIb productions of the Third Style, with parallels in the triclinium (p) of the House of Trebius Valens (III 2, 1) [27] or in the tablinum (7) of the House of M. Lucretius Fronto (V 4, a) [18] in Pompeii. We can also cite the case of San Gaetano di Vada near Volterra, although with the motifs around the entire panel from the final phase of the Third Style [28]. The frieze is decorated with Egyptian motifs and presents clear parallels between the production of the Third Style, such as that of the room (13) of the Casa dei Ceii (I 6, 15) [25] or that of the oecus (32) of the House of the Golden Bracelet (VI Ins. Occ., 42) [27].






Finally, the plant motifs on the cornice represent lotus flowers, although with a somewhat schematic execution, while the female head with a headdress has a very clear parallel dated to between the late Republican and Augustan periods in Rome, to which we can add another from Elea (Velia) [29]. This is a common motif in pre- and proto-Augustan productions, as we observe from its presence in the Arch of Augustus in the Roman Forum,

in a Campana relief in the House of Augustus in the Palatine [29] or in the *cubiculum* (b) of the Villa della Farnesina [30]. Its presence in our case corresponds to a subsequent continuity that is confirmed in paintings in a large number of examples [2,31]. The analysed elements allow a clear association with a Third Style Phase IIb production, which fits in well with the material context to which the fragments are associated and whose *terminus ante quem* is between 54 and 100 BC.

2. Materials and Methods

The fragments were initially examined under an optical microscope to distinguish layers, examine their microscopic properties and select appropriate areas for analysis. The combination of X-ray diffraction and X-ray fluorescence spectroscopy (XRD and XRF, respectively) and petrographic analysis provided information to determine the composition of the mortar. Finally, micro-Raman spectroscopy (μ -Raman) was used to reveal the chemical nature of the pigments. Table 1 shows the fragments analysed and the composition of the pigments and mortars.

Table 1. Fragments analysed and composition of pigments and mortars.

Photograph	Fragment	Reference	Macroscopic Colour	Compounds Found	Mortar Components
	F1	UE 1437	Black, Yellow, Blue, Green, White, Red	Carbon (C), Goethite (α -FeOOH), Egyptian blue ($\text{CaCuSi}_4\text{O}_{10}$), Glauconite ($(\text{Fe}^{3+}, \text{Al}, \text{Mg})_2(\text{Si}, \text{Al})_4\text{O}_{10}(\text{OH})_2$), Calcite (CaCO_3), Cinnabar (HgS).	Calcite; Quartz; Anorthite; Albite; Kaolinite
	F2	UE 1537	Black, Yellow, Blue, Green, White, Red	Carbon (C), Goethite (α -FeOOH), Egyptian blue ($\text{CaCuSi}_4\text{O}_{10}$), Glauconite ($(\text{Fe}^{3+}, \text{Al}, \text{Mg})_2(\text{Si}, \text{Al})_4\text{O}_{10}(\text{OH})_2$), Calcite (CaCO_3), Hematite (α -Fe ₂ O ₃), Minium (Pb ₃ O ₄ , PbO ₂)	Calcite; Quartz; Anorthite; Albite; Kaolinite
	F3	UE 1537	Black, Yellow, White, Red	Carbon (C), Goethite (α -FeOOH), Calcite (CaCO_3), Hematite (α -Fe ₂ O ₃), Minium (Pb ₃ O ₄ , PbO ₂)	Calcite; Quartz; Anorthite; Albite; Kaolinite
	F4	UE 1537	Black, Blue, Green, White, Red	Carbon (C), Egyptian blue ($\text{CaCuSi}_4\text{O}_{10}$), Glauconite ($(\text{Fe}^{3+}, \text{Al}, \text{Mg})_2(\text{Si}, \text{Al})_4\text{O}_{10}(\text{OH})_2$), Calcite (CaCO_3), Hematite (α -Fe ₂ O ₃), Minium (Pb ₃ O ₄ , PbO ₂)	Calcite; Quartz; Anorthite; Albite; Kaolinite
	F5	UE 785	Green, White, Red	Glauconite ($(\text{Fe}^{3+}, \text{Al}, \text{Mg})_2(\text{Si}, \text{Al})_4\text{O}_{10}(\text{OH})_2$), Calcite (CaCO_3), Hematite (α -Fe ₂ O ₃), Cinnabar (HgS).	Calcite; Quartz; Anorthite; Albite; Kaolinite

2.1. X-ray Diffraction

X-ray diffraction patterns were acquired using a Bruker D8 Advance diffractometer equipped with a goniometer and an automated DACO-MP recording system. The samples underwent irradiation with a copper K α line ($\lambda = 1.54 \text{ \AA}$). This instrument was equipped with a nickel filter and a graphite monochromator, operating at a goniometer speed of 2 degrees per minute. To increase homogeneity, samples were ground into smaller particles using an agate mortar. After this, they were placed on plastic slides and compressed to ensure that the exposed surface was as flat and uniform as possible.

2.2. X-ray Fluorescence

X-ray fluorescence (XRF) spectroscopy was used to determine and quantify the chemical elements in the mortar. The spectra were collected using a Rigaku ZSX Primus IV wavelength X-ray spectrometer, which features a 3 kW Rh-target X-ray tube, ten analyser crystals, a sealed proportional counter for the detection of light elements and a scintillation counter for heavy elements. Data were gathered at various points on the surface of each sample and then averaged.

2.3. Petrographic Analysis

The mineralogy and textural properties of samples were studied on 30 μm -thick polished thin sections using transmitted light microscopy at the Applied Petrology Laboratory (LPA-UA). Photomicrographs were performed by using a Zeis Axioscop petrographic microscope with a USB UI-1490SE digital camera.

2.4. Optical Microscopy

The target samples were visually examined at 100 \times magnification under a LEICA DCM8 Confocal Interferometric Microscope for Materials, whose 3D material surface metrology system allows for the study of rough surfaces through confocal microscopy.

2.5. Micro-Raman Spectroscopy

Micro-Raman spectra were acquired using a Renishaw InVia Raman Microscope, which includes a Leica microscope setup with various lenses, monochromators, a CCD camera and dual lasers (532 and 764 nm). The spectral data collection spanned a range from 140 to 1700 cm^{-1} , using the 532 nm green laser for excitation. To enhance the signal-to-noise ratio, the total number of scans was adjusted, and the laser power was carefully regulated to prevent any heat-induced chemical alterations in the pigments. Spectral analysis, including baseline adjustment and signal smoothing, was conducted using Renishaw's Wire v. 3.4 software.

To examine the existence of organic binders, a procedure was implemented to extract the paint layer from all fragments using a variety of organic solvents, including cyclohexane, dichloromethane and ethanol. Through this process, small quantities of paint (around 100–125 mg) were meticulously detached from the surface and immersed in the selected organic solvent for 24 h at ambient temperature. Subsequently, the solvent was filtered from the mixture and subjected to analysis via UV–Visible spectroscopy and gas chromatography–mass spectrometry.

3. Results

3.1. Mortar

The study of the mortar on which Roman wall paintings were applied is also of interest. As Vitruvius commented [32,33], the mortar was applied to walls and prepared to receive paint by first smoothing the walls to facilitate the coating with one or several layers, up to seven according to him, but more often only two or three are present. In our case, the fragments contained three preparatory layers of mortar and a finishing layer (Figure 5). This mortar was analysed using X-ray fluorescence (XRF) and X-ray diffraction (XRD). Table S1 shows the results of the XRF analysis for all samples expressed as a percentage of

oxides. The major components were calcium oxide and silicon oxide. In addition, other components, such as magnesium oxide and aluminium oxide, also appear in moderately high percentages, as does iron oxide. As Vitruvius indicates in his work, the mortars were prepared based on lime and sand. In some cases, hydraulic components were also added, primarily detected as iron and aluminium oxides. In our case, the percentages of such species detected in the mortars are relatively high and could point to the possibility that the mortar had a certain hydraulic character, although their origin may lie in the presence of feldspar sands and clay intrusions in mortars [32].

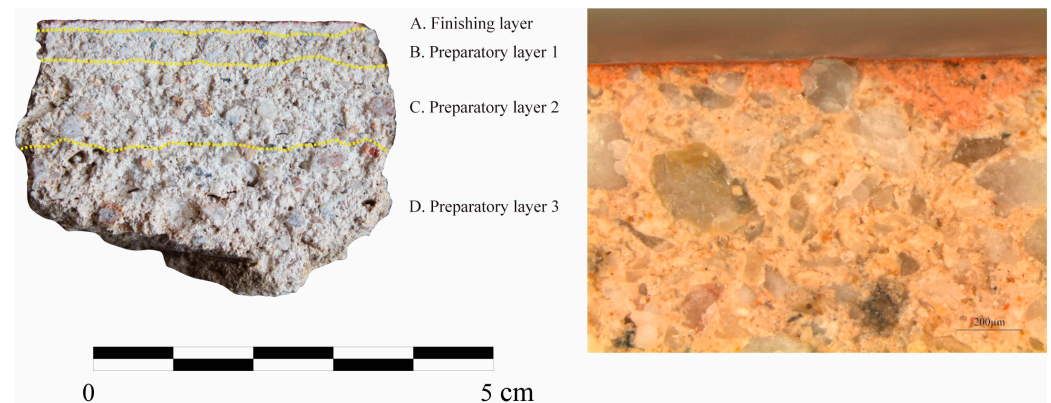


Figure 5. View of the stratigraphic sequence of the mortar layers in sample F5 and detail of the finishing layer under optical microscopy.

All the XRD patterns were similar in all fragments (Figure 6a,b) and are consistent with the majority presence of quartz (α -SiO₂, JCPDS No. 46-1045) and calcite (CaCO₃, JCPDS No. 05-0586). The additional peaks observed were assigned to anorthite, a calcium aluminosilicate Ca(Al₂Si₂O₈), albite, a sodium aluminosilicate NaAlSi₃O₈, both from the tectosilicate family, and kaolinite Al₂Si₂O₅(OH)₄, a phyllosilicate. These last silicates could be related to the use of ceramic materials in the preparation of hydraulic mortar [34].

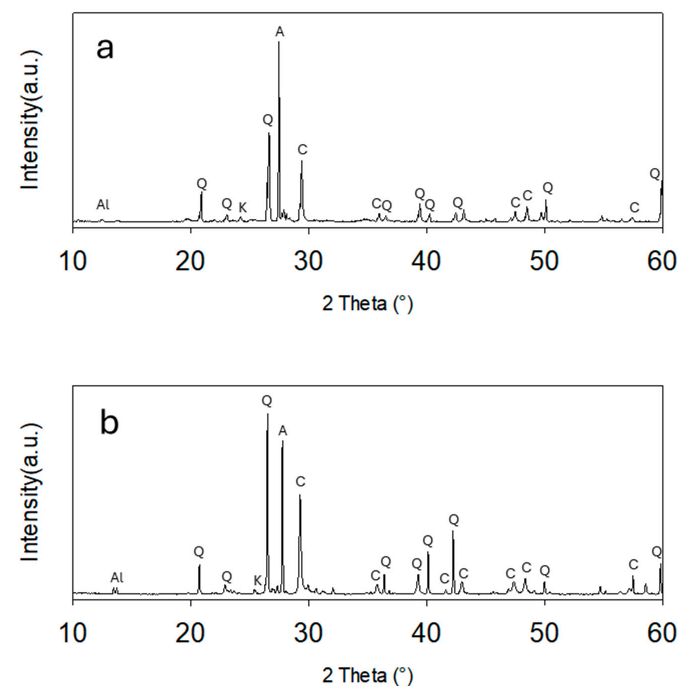


Figure 6. XRD patterns for the mortar: (a) F1, (b) F5. C: Calcite; Q: Quartz; A: Anorthite; Al: Albite; K: Kaolinite.

On the other hand, to complete the study of the mortar, binder and aggregate, it is also essential to observe a thin section. From the outside to the inside, four layers can be distinguished: A (finishing layer); B (preparatory layer 1); C (preparatory layer 2); D (preparatory layer 3). Mortar characterisation using optical microscopy shows a granular texture and a binder/aggregate ratio of around 1/3 in the inner layers (B, C, D) and slightly lower in the outermost and thinner layer (A) (binder/aggregate: 1/2) and at the top of the lower layers (binder/árido approx. 1/2.5). The aggregate centile is around 5–6mm. The colour of the binder is light.

The nature and sizes of the aggregate is very diverse. Quartz and feldspar grains and metamorphic rock fragments (quartzite, gneiss) predominate (Figures 7 and 8A,B). As minority components, fragments of metamorphic rock (phyllites, marbles) and sedimentary rock (breccias), opaque grains (rich in iron oxides), flints and micas can be distinguished. The size of the clasts or aggregates is very varied, from 50 μm to 6 mm. In the outer layer (A) the size range is smaller, from 25 μm to 2.5 mm. Most of the coarser clasts (rock fragments, quartz) as well as the smaller ones are generally angular to subangular. Clast size distribution (calibrated or sorted) is poor. They have no predominant orientation.

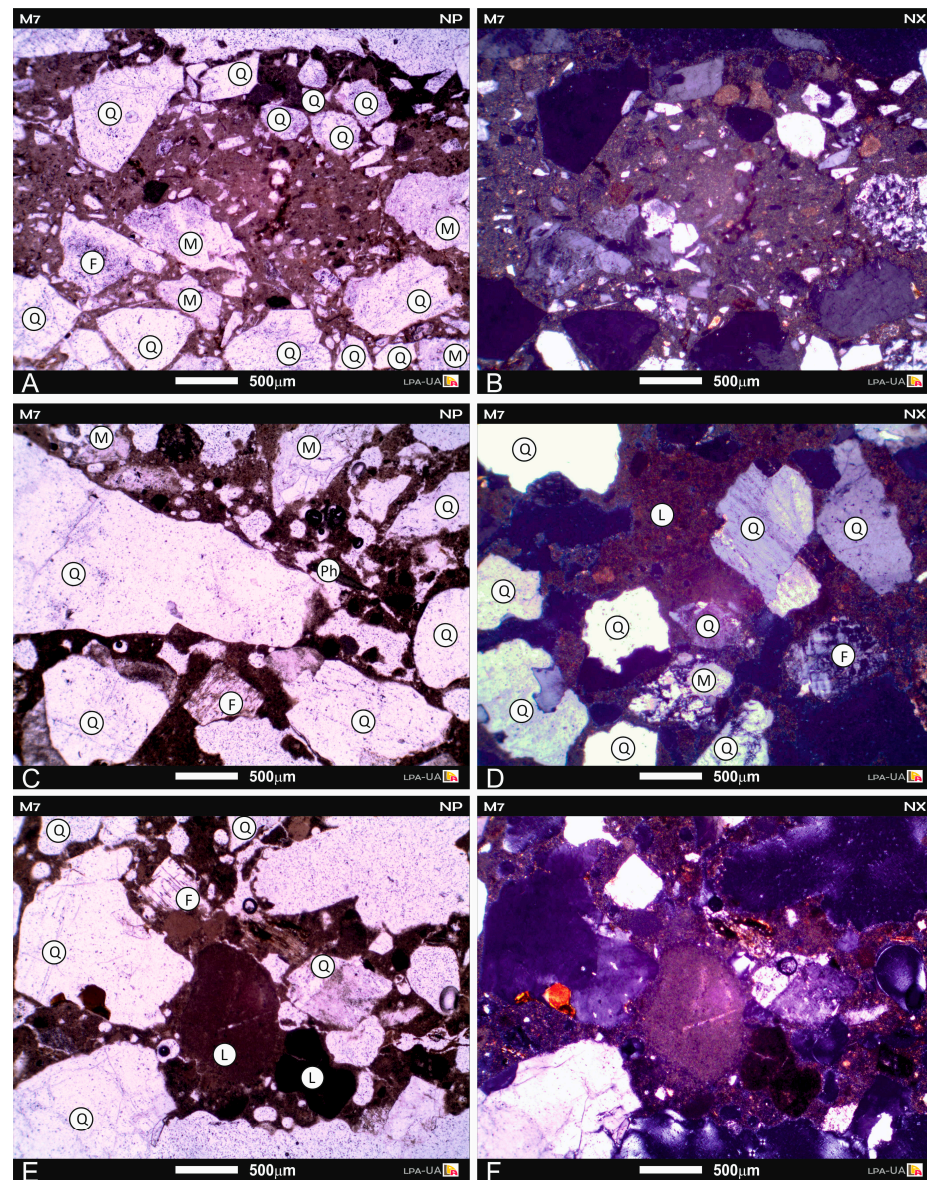


Figure 7. (A,B) General view of the A layer (finishing layer). Predominance of metamorphic rock fragments (quartzite) and quartz and feldspar grains in a micritic lime binder. (C,D) General view

of layer B (preparatory layer 1). Predominance of quartz grains and some feldspar grains and fragments of metamorphic rocks. Micritic lime binder. (E,F) Layer C (Preparatory layer 2). Detail of siliceous aggregates (quartz, feldspar) and calcareous granules (lime lumps). NP: parallel nicols; NX: crossed nicols; Q: quartz; F: feldspar; M: metamorphic rock fragment; Ph: phyllosilicates (micas); L: lime lumps.

As for the binder, it is a micritic lime binder composed mainly of calcium carbonate (calcite) and microcrystalline (micrite). Its texture and density is fairly homogeneous, of a lumpy type (Figure 8C,D). It has the presence of granules or particles attributable to nodules in the lime (lime lumps) (Figure 7D,F) and reaction rims in some aggregates. It has a low clay and iron oxide content (<5%).

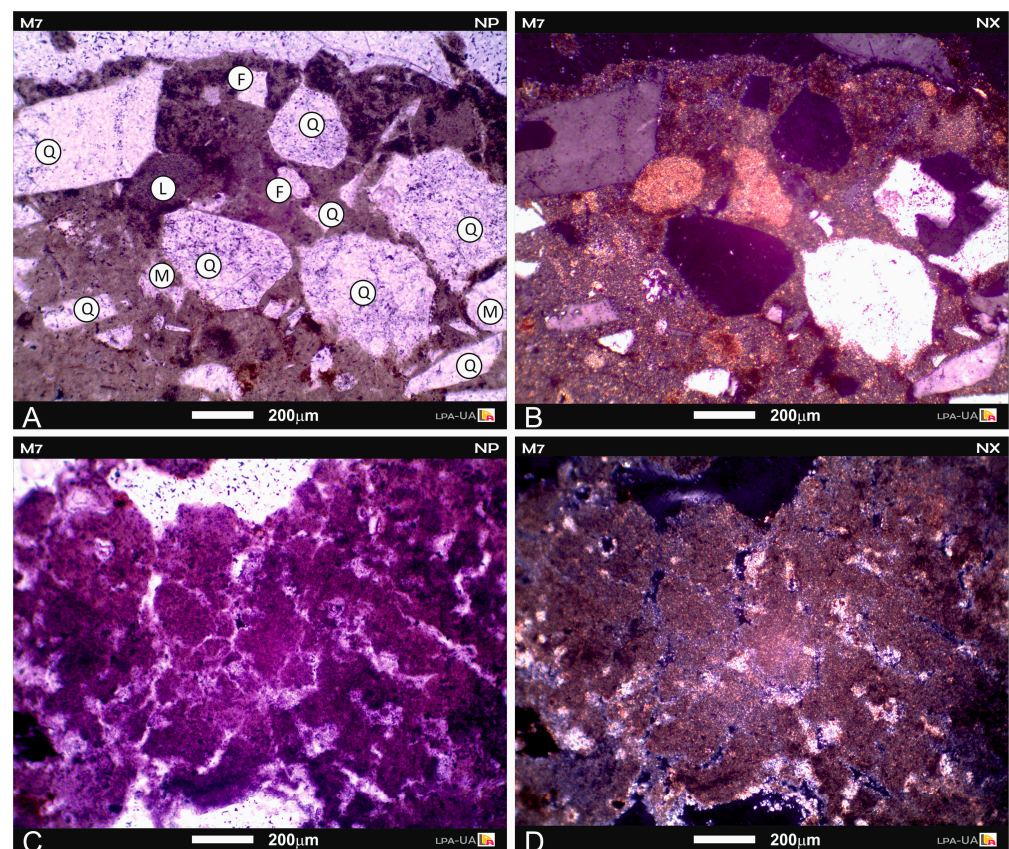


Figure 8. (A,B) General view of the D layer (preparatory layer 3). Siliceous aggregates (quartz, quartzite) and calcareous granules (lime lumps) (centre) in the binder. (C,D) Detail of the lumpy texture of the binder. NP: parallel nicols; NX: crossed nicols; Q: quartz; F: feldspar; M: metamorphic rock fragment; L: lime lumps.

The porosity is high, mainly intergranular, with vacuoles (20–150 μm) and fissures around the aggregates and calcareous granules (Figure 8C,D), probably widened by dissolution processes.

3.2. Surface Morphology

Figure 9 shows a representative image of a Blanes fragment observed through a Confocal Interferometric Microscope for Materials. Microscopy revealed the presence of various paint layers. Initially, a yellow base layer was applied over the plaster. This layer appears in all the degraded areas of the sample, where the surface pigment has been eroded over time. Subsequently, we can see how a layer of red, yellow, white and/or green pigment was applied, outlining the different decorations shown in the sample. These are represented with the base of the piece in yellow and the floral details in white and green. Furthermore,

we can observe how small blue particles appear in the green sample, a technique to enhance the brightness and tone of the colour amply described by authors such as Vitruvius. All of this led us to undertake a detailed analysis of the different pigments applied in the samples.

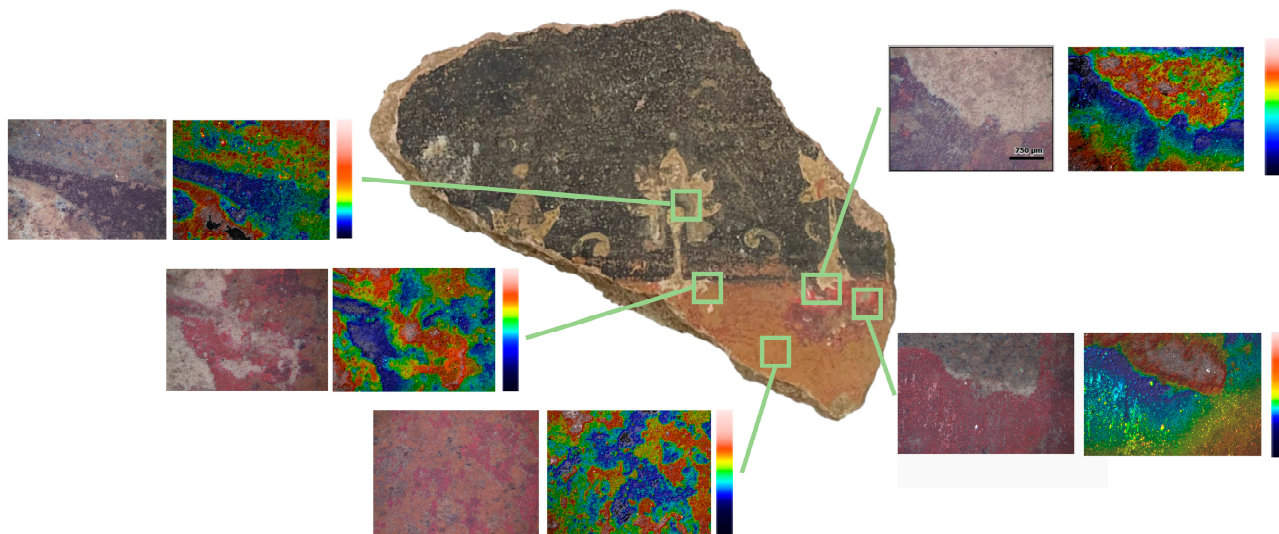


Figure 9. Representative image of a fragment observed through a Confocal Interferometric Microscope for Materials (the blue and red shades represent the deeper and outer areas of the sample, respectively).

3.3. Painting Techniques

During the ancient Roman period, artists used two main methods for the application of pigments: the fresco and secco painting techniques. Although all mural works are commonly referred to as frescos, regardless of their execution technique, the fresco method specifically required the application of colourants on still-moist lime mortar. In contrast, the secco technique was characterised by enhancing the fixation of pigments using an organic binder, such as egg, fat or resin, which often allowed for their direct application on a surface without the need for prior preparation with calcium carbonate or gypsum. Additionally, there was also a painting modality called encaustic, in which pigments were mixed with wax to optimise their adhesion.

The potential presence of organic binders in the samples was examined using the same analysis techniques as in other works [35,36]. However, none of the spectra contained signals of organic compounds potentially used as binders.

The microscope confirmed the previous visual findings, i.e., that some fragments contained overlapping pigment layers. It seems logical to assume that certain pigments, such as cinnabar and minium, were applied using the secco technique. This is consistent with Vitruvius' statement that considered certain pigments unstable in a strongly alkaline medium such as lime (De Architectura, VII).

3.4. Pigments

3.4.1. Black

This colour is found in the majority of samples; in all cases, the Raman spectra show the same profiles. Figure 10a illustrates the Raman spectrum corresponding to the use of black as the primary tone, applied to surfaces entirely covered by that colour. On the other hand, Figure 10b shows the Raman spectrum for cases where black is used in combination with other pigments, contributing a dark tone without being the predominant colour. In Roman times, carbon-based pigments were classified as bone black, carbon black and vine black, depending on how they were made. In all cases, the Raman spectra obtained at different points on the surface of the samples showed the same profile, displaying two broad bands at 1374 (D band) and 1583 cm^{-1} (G band) [37]. In particular cases, the

position, intensity and width of these bands provide structural information, allowing for discrimination between samples of different origins [38]. However, the relationship between the G:D band and its position does not allow discrimination between the three types of carbon mentioned above. The process of making bone black leaves a phosphate residue, which is always represented in a Raman signal at ca. 960 cm^{-1} corresponding to the symmetric stretching of P-O bonds in phosphate groups. Therefore, the presence of bone black can be ruled out, and the pigment must have been prepared from either carbon black or vine black. The latter, however, presents a hue with bluish undertones, which were not observed through microscopy, leading us to believe that the black pigment must have been obtained from carbon black [39].

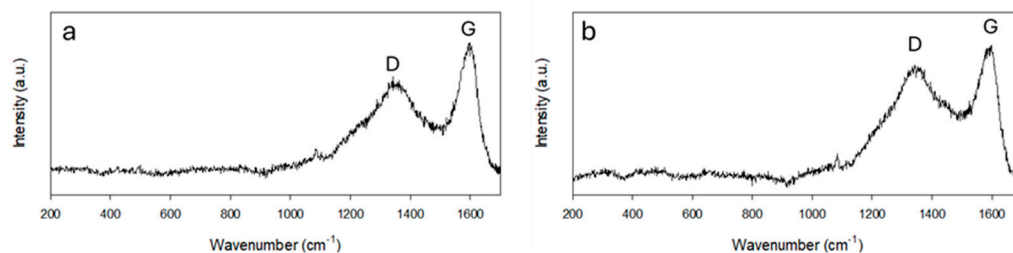


Figure 10. Raman spectra for black pigments. Black background (a) and black particles (b) on the surface.

3.4.2. Yellow

The yellow pigments commonly used in Roman times were obtained from yellow ochre due to its ubiquity in the earth's crust. Figure 11 shows one of the micro-Raman spectra obtained, where the yellow pigment in all cases contained goethite [$\alpha\text{-FeO(OH)}$] [40]. As can be seen, the spectrum corresponding to goethite displays the typical bands of this mineral at 246, 301, 387, 420, 482, 552, 687 and 998 cm^{-1} [41]. The fact that all these bands appear together denotes the fact that the purity of this pigment was very high. Additionally, the spectrum shown contains an intense band at 1084 cm^{-1} and two others at 712 and 276 cm^{-1} , all typical of calcite [42].

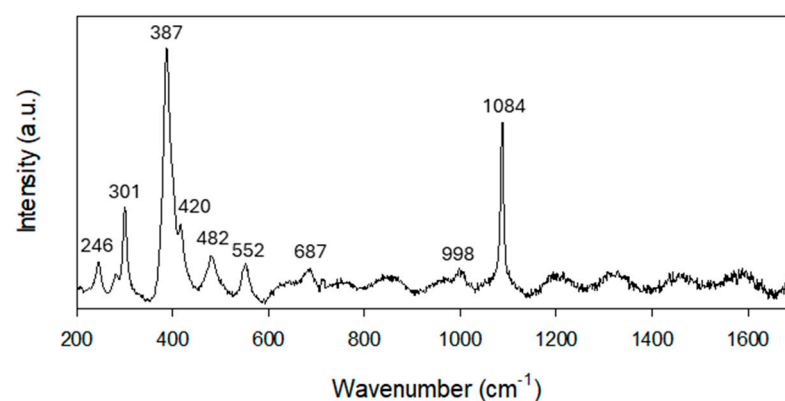


Figure 11. Raman spectrum for yellow paint layer.

3.4.3. Blue

The chemical nature of the blue pigment was unequivocally established by Raman spectroscopy. As can be seen in Figure 12, the Raman spectrum of the blue area contained an intense band at 429 cm^{-1} along with other bands of medium intensity at 1084, 984, 568 and 474 cm^{-1} . These bands, along with the rest of the minor bands, confirmed the presence of Egyptian blue [43]. In turn, the spectrum matches entirely with cuprorivaite, a mineral chemically identical to this compound. This pigment was typically prepared by heating a mixture of calcium (usually powdered limestone), a copper compound and silica (usually

sand) to about 850 °C, producing a compound with the formula $\text{CaCuSi}_4\text{O}_{10}$ known as “Egyptian blue” (caeruleum aegyptium) [44].

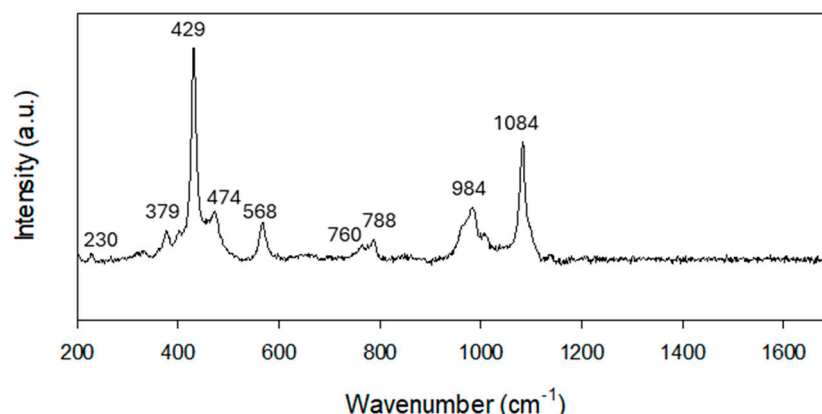


Figure 12. Raman spectra for blue paint layer. Experimental parameters.

3.4.4. Green

This pigment was observed in various areas of the samples representing different figurative details. The study of the green pigment using Raman spectroscopy suggests the use of green earth (creta viridis), a denomination reserved for two minerals: glauconite and celadonite. The presence of this green pigment in Hispania is well documented in various classical sources. Glauconite and celadonite are two similar mica minerals. Their chemical composition, $\text{K}(\text{Al}, \text{Fe}^{\text{III}})(\text{Fe}^{\text{II}}, \text{Mg})\text{O}_{10}(\text{OH})_2$, varies with ionic substitution. The Raman spectrum of the green samples was carried out to differentiate between these two very similar minerals [45]. The bands for glauconite and celadonite are described in the literature [46]. Green pigments are attributed to weak and broad bands. The bands described to differentiate between the green earths are divided into two sections. On the one hand, the Raman spectral region just below 600 cm^{-1} is examined, where a band assigned to the stretching vibrations of the Si-O bond in SiO_4 tetrahedra appears (at 550 cm^{-1} in celadonite and at 590 cm^{-1} in glauconite). On the other hand, there are less intense bands approximately between $260\text{--}280 \text{ cm}^{-1}$, which are useful for discriminating between celadonite (279 cm^{-1}) and glauconite (264 cm^{-1}). Figure 13a shows the Raman spectrum for the analysed green pigment, which contained a relatively intense band at 585 cm^{-1} and another of medium intensity at 265 cm^{-1} , thus assigning said pigment to glauconite [46]. Upon examining the surface of the green areas in the different fragments under the microscope, the presence of small blue areas was observed. Figure 13b shows a Raman spectrum performed in one of these blue areas, and we observed the presence of Egyptian blue. The presence of green earth (glauconite) and Egyptian blue is common in analysed samples from the Roman era. In fact, the Romans added a small amount of Egyptian blue to green earth to brighten its naturally dull colour [47,48].

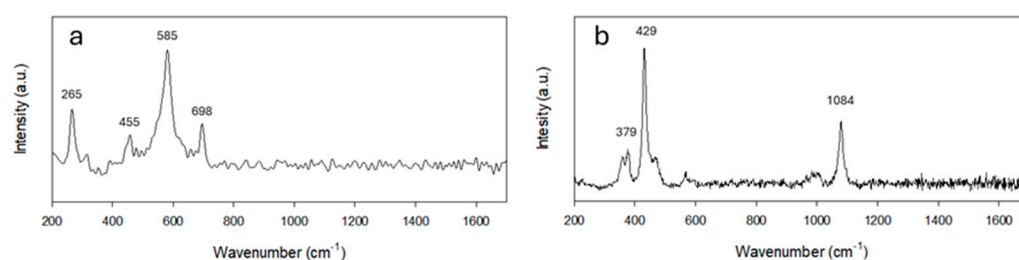


Figure 13. Raman spectra green layer. Green (a) and blue (b) particles on the green surface.

3.4.5. White

White is present in the decorative motif of the F2 y F3 samples, mixed with other pigments to vary the colour's hue. Figure 14 shows the spectrum of a white area; those of the other fragments were similar and are not shown. As can be observed, the spectrum has an intense band at 1090 cm^{-1} in addition to two smaller ones at 717 and 288 cm^{-1} ; these signals indicate that the pigment comes from calcium carbonate in the form of calcite [49].

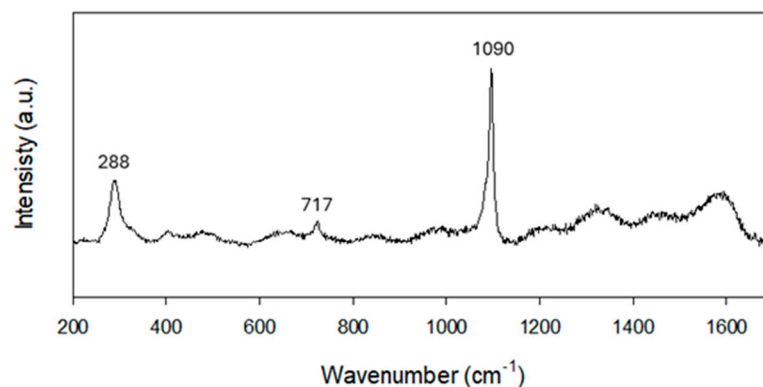


Figure 14. Raman spectra for the white zone.

3.4.6. Red

As can be seen in the photograph of the Figure 3 set assemblage, the samples show different shades of red. Thus, we can observe a dark red, another brighter one similar to vermilion and finally a lighter shade similar to orange. According to Roman authors, reddish pigments were mainly obtained from natural minerals such as hematite (Fe_2O_3), cinnabar (HgS) and minium (Pb_3O_4 , PbO_2) [32,50]. Table 1 provides a summary of the presence of different red colours in the analysed samples. Figure 15 shows the Raman spectra performed for each of the shades observed in the set. Firstly, we observed in the dark red spectral bands what can be attributed to the different modes of hematite ($\alpha\text{-Fe}_2\text{O}_3$) vibration (Figure 15a). The bands located at 291 , 408 and 611 cm^{-1} correspond to the symmetric Fe-O bending vibrations [41]. In addition, those observed at 222 and 499 cm^{-1} are assigned to the vibration modes of symmetric stretches, while the broad bands at 660 and 1319 cm^{-1} are also attributable to hematite [51,52]. Next, we observed a red area whose shade is brighter and whose spectral bands can be assigned to the different modes of vibration of cinnabar (HgS), known in classical texts as vermilion [32,50]. Figure 15b shows an intense band at 256 cm^{-1} and two smaller ones at 291 and 346 cm^{-1} , confirming that cinnabar was used for the bright red colour (vermilion) [53]. Finally, we observed the presence of a dark colour on an orange paint layer in certain areas of the set. The Raman spectrum for the orange area (Figure 15c) shows an intense band at 551 cm^{-1} along with other weaker bands at 228 , 482 and 1088 cm^{-1} attributable to red lead [54]. Interestingly, there was no difference in this spectrum between the dark and orange areas. Therefore, both pigments must be a lead-based compound. It is well described that most of the alterations of red lead (Pb_3O_4 , PbO) in paintings appear as a darkening or blackening of the pictorial layer [55,56]. During aging, it is assumed that the red lead alteration mechanisms depend on various factors, such as instability in light, humidity and microbial development. In all cases, the possibility was investigated that the alteration of the pigment in mural paintings may have been the result of the formation of various secondary phases. The main cause of the darkening of red lead in mural paintings consists of its transformation into black lead dioxide ($\beta\text{-PbO}_2$, plattnerite) [57].

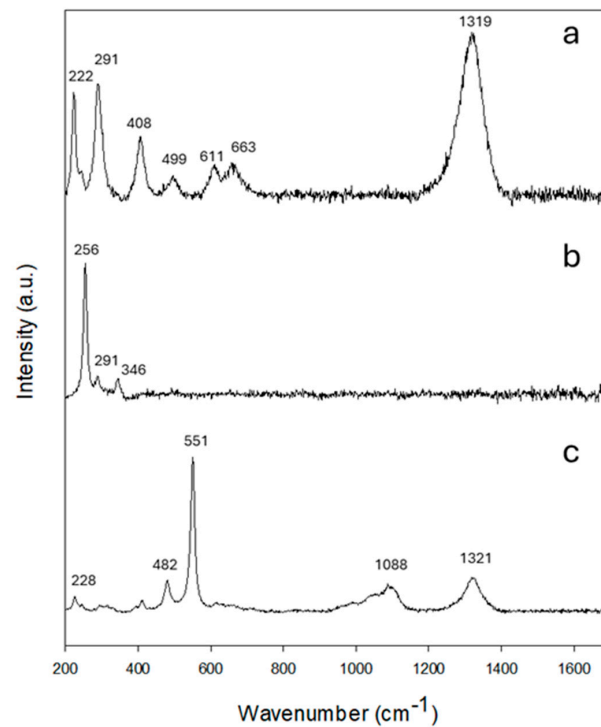


Figure 15. Raman spectra for the red zones. Haematites (a) cinnabar (b) and minium (c) on the red surface.

4. Discussion

The archaeometric study offers interesting data for a more in-depth exploration of the execution techniques and pigments used. It allows us to largely characterise a mural painting assemblage from Augusta Emerita dated to the first half of the 1st century AD. The data from the analysis of the mortar allow us to see certain particularities that show a workshop using a refined and carefully executed technique in accordance with what we observe in the stylistic study and that also links it with a workshop of Italic origin. Although the lime lumps in the mortar has been pointed out as evidence of poor lime slaking and poor working of the raw material [58], this is common in pre-industrial mortars. Therefore, given that their presence is not significant in our mortars, we do not believe they are indicative of poor lime working. In addition, the presence of marble crystals, although minor due to the partial loss of the finishing layer in the preparation of the sample, could be an indication of the artisan's intention to make it more solid or mechanically resistant and gives brightness to the surface. Vitruvius (*De Architectura*, VII, 3, 6) and Pliny (*Naturalis Historia*, XXXVI, 177) tell us of this technique, although there are few known examples in Hispania [59–61].

The majority presence of metamorphic rocks and quartz and feldspar grains shows that local materials were used to make the mortars. This can be seen from the geological map of the area around Mérida, which is located on a massif of amphibolites, feldspathic quartzites, graphite shales and metasandstones (Figure 16). However, this does not allow us to answer the question regarding the specific exploitation area, since the evidence of quartzite quarries and lime kilns dates back to the late Imperial period, with the earliest exploitation unknown. Direct extraction from the urban area itself cannot be ruled out, as confirmed by the exploitation of material documented in the dump on Cabo Verde Street, later filled with this waste [62]. From the point of view of the conservation and degradation of the mortars, it is worth highlighting the considerable compaction generally found in those of the early Imperial pictorial remains in Augusta Emerita. In this respect, the larger quartz content of the arid aggregates could explain the better conservation of the pictorial and stucco remains in Mérida. This can be seen from the studies carried out at other sites, such as Carthago Nova or Gades, with a majority composition of calcites [61].

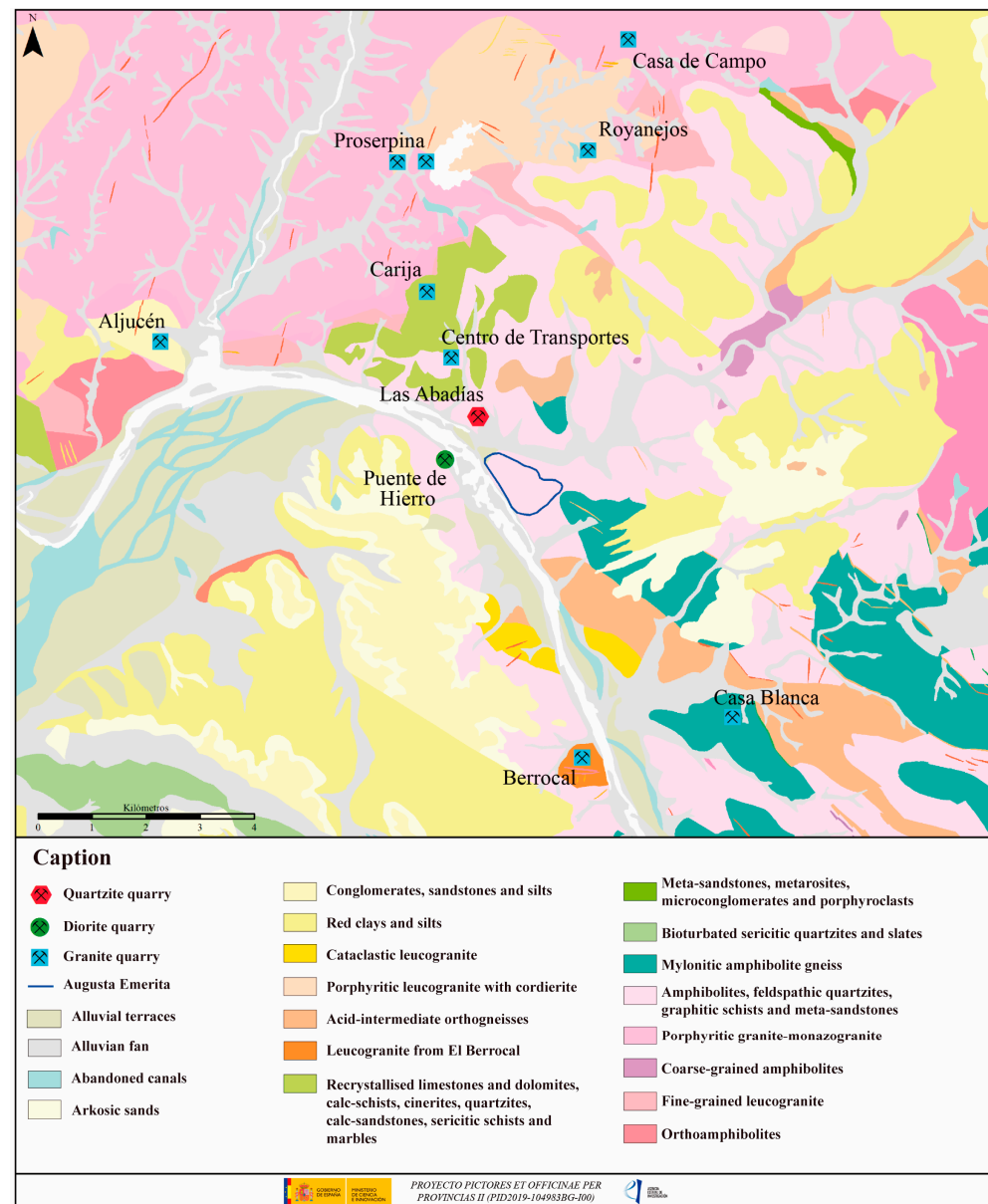


Figure 16. Geological map of Mérida and its surroundings.

The most interesting analysis comes from the study of the pigments. Although the data provided by Raman spectroscopy in relation to black, white, blue, yellow and green pigments do not differ from those generally documented in the Roman world, the last of these is shown to have been applied mixed with Egyptian blue crystals. This shows the use of a technique that we can document in a general fashion in the green pigments of late Republican and early Imperial productions with the aim of giving them a lighter, brighter tone [5,47]. However, we cannot rule out that this was an attempt to falsify malachite, as indicated by the sources (Pliny, *Naturalis Historia*, XXXIII, 86–91; XXXIV, 110–116 and XXXV, 30) and proposed for other assemblages [17].

As far as the red pigment is concerned, we were able to differentiate hematite with minium, cinnabar with a sublayer of goethite and cinnabar in fragments that correspond to three different panels. In the first case, this mixture is confirmed in Hispania in the House of the Red Columns in Sisapo, in groups of the Third Style-2nd century AD [63] and in Grau Vell, Sagunto in the 4th century AD [64]. Added to these are various works in the Italian area its reveal their presence in groups from the Hadrian's period [65]. The latter raise the possibility that it was a way of obtaining the pigment called sandyx in the sources

(Pliny, *Naturalis Historia*, XXXV, 20–23) (on the question of Latin terms see Becker [66], 2022, especially pages 7–11). Based on these indications, we can hypothesise an intention by the artisans to falsify the pigment or reduce costs, as suggested in the sources. This has also been indicated in relation to other groups in which the mixture of minium and cinnabar is documented [64].

As for the fragment with cinnabar and a sublayer of goethite, this solution appears more widely confirmed in pictorial production, with various cases in Hispania beginning in the late Republican period [64]. This again raises the question of identifying this technique as a way of reducing costs or protecting the cinnabar from degradation [67]. The variety of pigments indicates a careful and precise selection on the part of the artisans painting the panels, once again confirming the high technical quality and the wealth of the owner.

Most of the fragments in which only cinnabar is documented show blackening that could be the result of sulfation of the calcite in the mortar caused by exposure to the sun [68]. The observation of some fragments without blackening, the absence of sublayers and the use of cinnabar in large areas such as panels implies that it must have been applied using the fresco technique. In this case, a binder such as beeswax would probably have been used (Pliny, *Naturalis Historia*, XXXIII, 40), although this has not been documented. On the other hand, the absence of a sublayer on the fragments of the panel in which only cinnabar red is detected could be an indication of either the participation of different artisans in the execution of the panels or that the differences between them correspond to a mere cost-saving exercise for the rest of the panels. We should remember that the considerable price difference between cinnabar and hematite red would have been a significant handicap when it came to painting large areas on a wall with that pigment. This has also been confirmed by recent experimental archaeology studies [69].

5. Conclusions

The comprehensive study of the assemblage has allowed us to delve more deeply into the decorative tendencies in Augusta Emerita during the first half of the 1st century AD. It has revealed that Italic workshops participated in the execution of its decorative schemes and motifs and that they were carried out with great technical precision.

The measured use of pigments for the panels in the middle zone suggests that this assemblage decorated an important area of the building it originally came from, given the use of cinnabar not only in small motifs on the frieze but also in large spaces such as the panels. In this respect, the use of other pigments either mixed or in sublayers for the rest of the panels would undoubtedly have sought to create a homogeneous image of the middle zone of the wall that would have evidenced a high economic status.

Supplementary Materials: The following supporting information can be downloaded at: <https://www.mdpi.com/article/10.3390/heritage7060129/s1>, Table S1. Chemical composition of the fragment determined by X-ray fluorescence (XRF) spectroscopy.

Author Contributions: G.C.A. and A.F.D. performed the archaeological analyses. J.R.R.A., D.C.H. and G.C.A. conducted the XRD, μ -Raman and chemical analyses. All authors have read and agreed to the published version of the manuscript.

Funding: Grant FJC2021-046548-I funded by MICIU/AEI/10.13039/501100011033 and by the European Union NextGenerationEU/PRTR; Project PID2019-104983GB-I00 funded by MICIU/AEI/10.13039/501100011033; Project PID2019-105376GB-C43 funded by MICIU/AEI/10.13039/501100011033.

Data Availability Statement: The authors declare that the manuscript is original, has not been submitted or published in any other journal and the data in the manuscript are real.

Acknowledgments: The authors are also grateful to the Consorcio Ciudad Monumental de Mérida, the director of the archaeological museum of Badajoz and the Professor Macarena Bustamante of the University of Granada. The authors are grateful to the Research Group PAI FQM-346, IQUEMA and the Central Research Support Service (SCAI) of the University of Córdoba for their help with the experimental part. D. C. acknowledges the FEDER funds for Programa Operativo Fondo Social Europeo (FSE) de Andalucía (PP2F_L1_07).

Conflicts of Interest: The authors declare no conflicts of interest.

References

1. Nogales Basarrate, T. Colonia Augusta Emerita. In *Ciudades Romanas e Hispania. I.*; Nogales Basarrate, T., Ed.; L'Erma di Bretschneider: Roma, Italy, 2021.
2. Heras Mora, F.J.; Fernández Díaz, A.; Bustamante Álvarez, M. Decoración Parietal de Augusta Emerita. Repertorio pictórico y contexto arqueológico a partir de las excavaciones de un vertedero del Suburbio Norte. In *Antike Malerei Zwischen Lokalstil und Zeitsil. Akten des XI Internationalen Kolloquiums der AIPMA*; Zimmermann, N., Ed.; Osterreichischen Akademie der Wissenschaften: Viena, Austria, 2015; pp. 461–472.
3. Castillo Alcántara, G. *Pictura Ornamentalis Romana. Análisis y Sistematización de la Decoración Pictórica y en Estuco de Augusta Emerita*; University of Murcia: Murcia, Spain, 2021.
4. Castillo Alcántara, G.; Fernández Díaz, A. El programa decorativo de la casa del Mitreo: Pintura, relieve y estuco. In *La Casa del Mitreo de Augusta Emerita*; Bejarano Osorio, A.M., Bustamante Álvarez, M., Eds.; Consorcio Ciudad Monumental de Mérida. Memoria 3; Monografías Arqueológicas de Mérida: Mérida, Spain, 2023; pp. 241–322.
5. Cerrato, E.J.; Íñiguez Berrozpe, L.; Cosano Hidalgo, D.; Guiral Pelegrín, C.; Ruiz Arrebola, J.R. Multi-Analytical Identification of a Painting Workshop at the Roman Archaeological Site of Bilbilis (Saragossa, Spain). *J. Archaeol. Sci. Rep.* **2021**, *38*, 103108. [[CrossRef](#)]
6. Castillo Alcántara, G.; Fernández Díaz, A.; Cosano Hidalgo, D.; Ruiz Arrebola, J.R. A Compositional and Archaeometric Study of the Third Pompeian Style Located at the Mons Saturnus of Carthago Nova (Cartagena, España). *J. Archaeol. Sci. Rep.* **2022**, *46*, 103670. [[CrossRef](#)]
7. Coutelas, A. Le Mortier de Chaux Dans La Peinture Murale Gallo-Romaine: L'apport Des Analyses à La Compréhension d'un Patrimoine Technique Ancien. In *La peinture Murale Antique: Méthodes et Apports d'une Approche Technique. Atti del Colloquio Internazionale Louvain-la-Neuve 21 Aprile 2017*; Cavalieri, M., Tomassini, P., Eds.; Quasar: Roma, Italy, 2021; pp. 149–160.
8. Brecoulaki, H.; Verri, G.; Kalaitzi, M.; Maniatis, Y.; Lilimpaki-Akamati, M. Investigating Colors and Techniques on the Wall Paintings of the 'Tomb of the Philosophers', an Early Hellenistic Macedonian Monumental Cist Tomb in Pella (Macedonia, Greece). *Heritage* **2023**, *6*, 5619–5647. [[CrossRef](#)]
9. Dilaria, S.; Sbrolli, C.; Mosimann, F.S.; Favero, A.; Secco, M.; Santello, L.; Salvadori, M. Production Technique and Multi-Analytical Characterization of a Paint-Plastered Ceiling from the Late Antique Villa of Negrar (Verona, Italy). *Archaeol. Anthropol. Sci.* **2024**, *16*, 74. [[CrossRef](#)]
10. Heras Mora, F.J.; Bustamante Álvarez, M.; Olmedo Grajera, A.B. El vertedero del Suburbio Norte de Augusta Emerita. Reflexión sobre la dinámica topográfica en el solar de la Calle Almendralejo N° 41. In *La gestión de los Residuos Urbanos en Hispania. Xavier Dupré Raventós (1956–2006). In Memoriam*; Remolà Vallverdú, J.A., Acero Pérez, J., Eds.; Anejos de Archivo Español de Arqueología, LX: Mérida, Spain, 2011; pp. 345–360.
11. Álvarez Martínez, J.M. Los accesos a la Colonia Augusta Emerita. La Puerta del Puente. In *Puertas de Ciudades. Tipo Arquitectónico y Forma Artística. Actas del Coloquio en Toledo del 25 a 27 de Septiembre de 2003*; Schattner, T., Valdés Fernández, F., Eds.; Verlag Philipp von Zabern: Mainz/Rhein, Germany, 2006; pp. 221–251.
12. Bustamante Álvarez, M. *La Terra Sigillata Hispánica en Augusta Emerita: Estudio Tipocronológico a Partir de los Vertederos del Suburbio Norte*; Anejos de Archivo Español de Arqueología, LXV: Madrid, Spain, 2013.
13. Heras Mora, F.J.; Olmedo Grajera, A.B.; Perez Maestro, C. Dinámica urbana en el Suburbio Norte de Augusta Emerita: Síntesis diacrónica de las excavaciones en el llamado Corralón de Los Blanes. *Mérida Excavaciones Arqueol.* **2017**, *12*, 707–745.
14. Márquez Pérez, J. *Los Columbarios: Arquitectura y Paisaje Funerario En Augusta Emerita*; Inst. de Arqueología de Mérida: Mérida, Spain, 2006.
15. Bustamante Álvarez, M.; Olmedo Grajera, A.B. De las cupae emeritenses: Nuevos datos estratigráficos. In *Las Cupae Hispanas: Origen, Difusión, Uso, Tipología*; Andreu Pintado, J., Ed.; Serie Monografías Los Bañales: Zaragoza, Spain, 2012; pp. 369–392.
16. Barbet, A. *La peinture murale en Gaule romaine*; Picard: Paris, France, 2008.
17. Íñiguez Berrozpe, L. *La Pintura Mural Romana de Ámbito Doméstico en el Conventus Caesaraugustanus Durante el Siglo I d.C. Talleres y Comitentes*; University of Zaragoza: Zaragoza, Spain, 2014.
18. Bastet, F.L.; De Vos, M. *Il Terzo Stile Pompeiano*; Nederlands Instituut te Rome: La Haya, The Netherlands, 1979.
19. Barbet, A. La diffusion du III style pompéien en Gaule: Première partie. *Gallia* **1982**, *40*, 53–82. [[CrossRef](#)]
20. Mazzoleni, D.; Pappalardo, U. *Domus: Pittura e Architettura D'illusione Nella Casa Romana*; Arsenal: San Giovanni Lupatoto, Italy, 2004.
21. Barbet, A.; Bujard, S.; Dagand, P.; Lefèvre, J.-F.; Maleyre, I.; Amadei, B.; Lemoigne, L. Peintures de Périgueux. Édifice de La Rue Des Bouquets Ou La Domus de Vésone. *Aquitania* **2008**, *24*, 42–76. [[CrossRef](#)]
22. Mostalac Carrillo, A.; Guiral Pelegrín, C. Preliminares sobre el repertorio ornamental del III y IV estilos pompeyanos en la pintura romana de España. *Itálica* **1990**, *18*, 155–173.
23. Mostalac Carrillo, A. La pintura romana en España: Estado de la cuestión. *Anu. Del Dep. De Hist. Y Teoría Del Arte* **1992**, *4*, 9–22.
24. Fernández Díaz, A. *La Pintura Mural Romana de Carthago Nova: Wvolución del Programa Pictórico a Través de los Estilos, Talleres y Otras Técnicas Decorativas*; Museo Arqueológico de Murcia; Monografías, 2: Murcia, Spain, 2008.
25. Barbet, A. La Peinture Murale Romaine. In *Les Styles Décoratifs Pompéiens (Segunda Edición)*; Picard: Paris, France, 2009.

26. Fagioli, F. La “riscoperta” degli intonaci dipinti dalle domus di via Sigismondo a Rimini: Nuovi dati dai depositi. In *Pictor 8. Peintures et Stucs D'époque Romaine. Études Toichographologiques*; Boislève, J., Monier, F., Eds.; Ausonius Éditions: Burdeos, France, 2020; pp. 315–322.
27. PPM = Pompei. In *Pitture e Mosaici. I-IX. (1990–2003)*; Istituto Della Enciclopedia Italiana: Roma, Italy, 1990–2003.
28. Benetti, I.; Donati, F.; Menchelli, S.; Pasquinucci, M.; Sangriso, P. Indagine Sulla Diffusione Del Terzo Stile in Etruria: Il Caso Di Vada Volaterrana. In *Pictores per Provincias II—Status Quaestionis. Actes du 13e Colloque de L'association Internationale pour la Peinture Murale Antique (AIPMA)*; Dubois, Y., Niffeler, U., Eds.; Antiqua: Basilea, Switzerland, 2018; Volume 55, pp. 555–565.
29. Cenci, C.; Lauria, M.; Violante, S. Decorazioni architettoniche e figurate in stucco. In *Evan Gorga. La Collezioni di Archeologia*; Capodiferro, A., Ed.; Museo Nazionale Romano: Roma, Italy, 2013; pp. 122–150.
30. Bragantini, I.; De Vos, M. Le decorazioni della villa romana della Farnesina. Museo Nazionale Romano. In *Le Pitture II, 1*; De Luca: Roma, Italy, 1982.
31. Benetti, I. Gorgoneia o teste di luna: Un aproccio terminologico al motivo ornamentale. In *AIRPA 2. Sistemi Decorativi Della Pittura Antica: Funzione e Contesto. Atti del II Coloquio AIRPA (Pisa, 2018)*; Donati, F., Benetti, I., Eds.; Quasar: Roma, Italy, 2020; pp. 217–228.
32. Vitruvio, M. *Los X Libros de Arquitectura de Marco Vitruvio Polión*; Cicon edic.: Cáceres, Spain, 1999.
33. Salvadori, M.; Sbrilli, C. Wall Paintings through the Ages: The Roman Period—Republic and Early Empire. *Archaeol. Anthropol. Sci.* **2021**, *13*, 187. [[CrossRef](#)]
34. Franquelo, M.L.; Robador, M.D.; Ramírez-Valle, V.; Durán, A.; Jiménez de Haro, M.C.; Pérez-Rodríguez, J.L. Roman ceramics of hydraulic mortars used to build the mithraeum house of Merida (Spain). *J. Therm. Anal. Calorim.* **2008**, *92*, 331–335. [[CrossRef](#)]
35. Cerrato, E.J.; Cosano Hidalgo, D.; Esquivel Merino, D.; Otero, R.; Jiménez-Sanchidrián, C.; Ruiz Arrebola, J.R. A Multi-Analytical Study of a Wall Painting in the Satyr Domus in Córdoba, Spain. *Spectrochim. Acta A Mol. Biomol. Spectrosc.* **2020**, *232*, 118148. [[CrossRef](#)] [[PubMed](#)]
36. Cerrato, E.J.; Cosano Hidalgo, D.; Esquivel Merino, D.; Jiménez-Sanchidrián, C.; Ruiz Arrebola, J.R. Spectroscopic Analysis of Pigments in a Wall Painting from a High Roman Empire Building in Córdoba (Spain) and Identification of the Application Technique. *Microchem. J.* **2021**, *168*, 106444. [[CrossRef](#)]
37. Wang, Y.; Alsmeyer, D.C.; McCreery, R.L. Raman Spectroscopy of Carbon Materials: Structural Basis of Observed Spectra. *Chem. Mater.* **1990**, *2*, 557–563. [[CrossRef](#)]
38. Caggiani, M.C.; Colomban, P. Raman Identification of Strongly Absorbing Phases: The Ceramic Black Pigments. *J. Raman Spectrosc.* **2011**, *42*, 839–843. [[CrossRef](#)]
39. Coccato, A.; Jehlicka, J.; Moens, L.; Vandenabeele, P. Raman Spectroscopy for the Investigation of Carbon-Based Black Pigments. *J. Raman Spectrosc.* **2015**, *46*, 1003–1015. [[CrossRef](#)]
40. Amadori, M.L.; Barcelli, S.; Poldi, G.; Ferrucci, F.; Andreotti, A.; Baraldi, P.; Colombini, M.P. Invasive and Non-Invasive Analyses for Knowledge and Conservation of Roman Wall Paintings of the Villa of the Papyri in Herculaneum. *Microchem. J.* **2014**, *118*, 183–192. [[CrossRef](#)]
41. De Faria, D.L.A.; Venâncio Silva, S.; De Oliveira, M.T. Raman Microspectroscopy of Some Iron Oxides and Oxyhydroxides. *J. Raman Spectrosc.* **1997**, *28*, 873–878. [[CrossRef](#)]
42. Gunasekaran, S.; Anbalagan, G. Spectroscopic Characterization of Natural Calcite Minerals. *Spectrochim. Acta A Mol. Biomol. Spectrosc.* **2007**, *68*, 656–664. [[CrossRef](#)]
43. Prieto-Taboada, N.; Fdez-Ortiz de Vallejuelo, S.; Santos, A.; Veneranda, M.; Castro, K.; Maguregui, M.; Morillas, H.; Arana, G.; Martellone, A.; de Nigris, B.; et al. Understanding the Degradation of the Blue Colour in the Wall Paintings of Ariadne's House (Pompeii, Italy) by Non-Destructive Techniques. *J. Raman Spectrosc.* **2021**, *52*, 85–94. [[CrossRef](#)]
44. Pagès-Camagna, S.; Colinar, S.; Couprie, C. Fabrication Processes of Archaeological Egyptian Blue and Green Pigments Enlightened by Raman Microscopy and Scanning Electron Microscopy. *J. Raman Spectrosc.* **1999**, *30*, 313–317. [[CrossRef](#)]
45. Jorge-Villar, S.E.; Edwards, H.G.M. Green and Blue Pigments in Roman Wall Paintings: A Challenge for Raman Spectroscopy. *J. Raman Spectrosc.* **2021**, *52*, 2190–2203. [[CrossRef](#)]
46. Moretto, L.M.; Orsega, E.F.; Mazzocchin, G.A. Spectroscopic Methods for the Analysis of Celadonite and Glauconite in Roman Green Wall Paintings. *J. Cult. Herit.* **2011**, *12*, 384–391. [[CrossRef](#)]
47. Mazzocchin, G.A.; Agnoli, F.; Mazzocchin, S.; Colpo, I. Analysis of Pigments from Roman Wall Paintings Found in Vicenza. *Talanta* **2003**, *61*, 565–572. [[CrossRef](#)] [[PubMed](#)]
48. Perez-Rodríguez, J.L.; de Haro, M.d.C.J.; Siguenza, B.; Martínez-Blanes, J.M. Green Pigments of Roman Mural Paintings from Seville Alcazar. *Appl. Clay Sci.* **2015**, *116*, 211–219. [[CrossRef](#)]
49. Gunasekaran, S.; Anbalagan, G.; Pandi, S. Raman and Infrared Spectra of Carbonates of Calcite Structure. *J. Raman Spectrosc.* **2006**, *37*, 892–899. [[CrossRef](#)]
50. Plinio, C. *Historia Natural de Cayo Plinio Segundo*. In *Traducido Por Francisco Hernández y Jerónimo de Huerta*; VISOR: Madrid, Spain, 1998.
51. Pailhé, N.; Wattiaux, A.; Gaudon, M.; Demourgues, A. Impact of Structural Features on Pigment Properties of α -Fe₂O₃ Haematite. *J. Solid State Chem.* **2008**, *181*, 2697–2704. [[CrossRef](#)]
52. Chamritski, I.; Burns, G. Infrared- And Raman-Active Phonons of Magnetite, Maghemite, and Hematite: A Computer Simulation and Spectroscopic Study. *J. Phys. Chem. B* **2005**, *109*, 4965–4968. [[CrossRef](#)]

53. Scheuermann, W.; Ritter, G.J. Raman Spectra of Cinnabar (HgS), Realgar (As₄S₄) and Orpiment (As₂S₃). *Z. Fur Naturforschung—Sect. A J. Phys. Sci.* **1969**, *24*, 408–411. [[CrossRef](#)]
54. Smith, D.C.; Barbet, A. A Preliminary Raman Microscopic Exploration of Pigments in Wall Paintings in the Roman Tomb Discovered at Kertch, Ukraine, in 1891. *J. Raman Spectrosc.* **1999**, *30*, 319–324. [[CrossRef](#)]
55. Aze, S.; Delaporte, P.; Vallet, J.M.; Detalle, V.; Grauby, O.; Baronnet, A. Towards the Restoration of Darkened Red Lead Containing Mural Paintings: A Preliminary Study of the β -PbO₂ to Pb₃O₄ Reversion by Laser Irradiation. In Proceedings of the International Conference LACONA VII, Madrid, Spain, 17–21 September 2007; Castillejo, M., Moreno, P., Oujja, M., Radvan, R., Ruiz, J., Eds.; CRC Press: London, UK, 2008; pp. 11–13.
56. Aze, S.; Vallet, J.M.; Detalle, V.; Grauby, O.; Baronnet, A. Chromatic Alterations of Red Lead Pigments in Artworks: A Review. *Phase Transit.* **2008**, *81*, 145–154. [[CrossRef](#)]
57. Burgio, L.; Clark, R.J.H.; Firth, S. Raman Spectroscopy as a Means for the Identification of Plattnerite (PbO₂), of Lead Pigments and of Their Degradation Products. *Analyst* **2001**, *126*, 222–227. [[CrossRef](#)] [[PubMed](#)]
58. Guiral Pelegrín, C.; Coutelas, A.; Íñiguez Berrozpe, L.; Muñoz Rufo, V.; Puertas López, C. Las pinturas de la domus de Can Cruzate de Iluro (Mataró, Barcelona). Estudio técnico y decorativo. *Pyrenae* **2023**, *54*, 133–158.
59. Dominguez-Bella, S.; Gener Basallote, J.M.; Kakoulli, I.; Jurado Fresnadillo, G.; Durante Macias, A. Informe de la actuación “Arqueometría del patrimonio histórico de Cádiz: Las pinturas romanas de la Neápolis gaditana. estudio de las pinturas murales y estucos de la c/Santa María N° 17–19 (Cádiz)”. *Anu. Arqueol. De Andal.* **2003**, *2*, 119–129.
60. Guiral Pelegrín, C.; Martín-Bueno, M.; Bilbilis, I. *Decoración Pictórica y Estucos Ornamentales*; Institución Fernando el Católico: Zaragoza, Spain, 1996.
61. Fernández Díaz, A.; Castillo Alcántara, G.; Alias Linares, A.; Lazón Torres, M.; Bernal Casasola, D.; Vargas Girón, J. De Gades a Carthago Nova: Análisis fisicoquímicos de morteros y restos pictóricos en dos enclaves costeros peninsulares. In *La Pintura Romana en Hispania. Del Estudio de Campo a su Puesta en Valor*; Fernández Díaz, A., Castillo Alcántara, G., Eds.; Editum: Murcia, Spain, 2020; pp. 295–313.
62. Pérez Maestro, C. Un área de Vertedero/Puticulum de época altoimperial localizada extramuros en la zona Noreste de la ciudad. Intervención arqueológica realizada en el solar situado en la Calle Cabo Verde s/n (Mérida). *Merida. Excavaciones Arqueol.* **2007**, *2004*, 153–170.
63. Zorzalejos Prieto, M.; Guiral Pelegrín, C.; Mansilla Plaza, L.; Palero Fernández, F.J.; Esbrí Víctor, J.M. Caracterización de pigmentos rojos en las pinturas de Sisapo (Ciudad Real, España). In *Antike Malerei Zwischen Lokalstil und Zeitsil. Akten des XI Internationalen Kolloquiums der AIPMA*; Zimmermann, N., Ed.; Österreichischen Akademie der Wissenschaften: Viena, Austria, 2015; pp. 607–614.
64. Guiral Pelegrín, C.; Íñiguez Berrozpe, L. El cinabrio en la pintura romana de Hispania. In *El oro rojo en la Antigüedad: Perspectivas de Investigación Sobre los Usos y Aplicaciones del Cinabrio Entre la Prehistoria y el fin del Mundo Antiguo*; Zorzalejos Prieto, M.M., Hevia Gómez y, P., Mansilla Plaza, L., Eds.; UNED-Universidad Nacional de Educación a Distancia: Madrid, Spain, 2020; pp. 337–372.
65. Fermo, P.; Piazzalunga, A.; De Vos, M.; Andreoli, M. A Multi-Analytical Approach for the Study of the Pigments Used in the Wall Paintings from a Building Complex on the Caelian Hill (Rome). *Appl. Phys. A* **2013**, *113*, 1109–1119. [[CrossRef](#)]
66. Becker, H. Pigment Nomenclature in the Ancient Near East, Greece, and Rome. *Archaeol. Anthropol. Sci.* **2022**, *14*, 20. [[CrossRef](#)]
67. Allag, C.; Grotembril, S. Le rôle des sous-couches. In *La Peinture Murale Antique: Méthodes et Apports d'une Approche Technique. Acti del Colloquio International Louvain-la-Neuve 21 Aprile 2017*; Cavalieri, M., Tomassini, P., Eds.; Quasar: Roma, Italy, 2021; pp. 205–212.
68. Terrapon, V.; Béarat, H. A Study of Cinnabar Blackening: New Approach and Treatment Perspective. In Proceedings of the 7th International Conference on Science and Technology in Archaeology and Conservation at Petra, Petra, Jordan, 7–11 December 2010; pp. 1–11.
69. Becker, H. Painting Aquae Sextiae Red: The Economic Choices of Painting with Red Ochre and Cinnabar. In *Proceedings of AIPMA XV*; Fernández Díaz, A., Castillo Alcántara, G., Eds.; Editum: Murcia, Spain, in press.

Disclaimer/Publisher’s Note: The statements, opinions and data contained in all publications are solely those of the individual author(s) and contributor(s) and not of MDPI and/or the editor(s). MDPI and/or the editor(s) disclaim responsibility for any injury to people or property resulting from any ideas, methods, instructions or products referred to in the content.